A Visi-coil Fiducial Markers Detection Method on kV Projection Images during Prostate Radiation Therapy

Shirin Badiei, Ling Zhuang, Jia Li

***Abstract*-Here an accurate automated method based on fast marching approach for detecting visi-coil fiducial markers by using kV imaging is presented. Visi-coil segmentation in each kV image is performed on one marker at a time via fast marching method which requires user input of the endpoints. Initially, a 3D model was extracted by thresholding CT images and is used here as reference. The reference 3D model is re-projected onto the kV images. The new 2D re-projection points provide information about the direction of the markers and zones within which each marker endpoint may lie. This information is employed to detect the start and end point of each visi-coil and remove user input in the fast marching method. A 3D reconstruction of the markers is computed from the segmentation results. The proposed automated visi-coil detection algorithm can increase accuracy of marker location on noisy images and when obscured by boney tissue.**

I. Introduction

Precise tumor localization during prostate cancer radiation therapy particularly in the case of hypo-fractioned dose delivery can optimize results by ensuring delivery of the correct radiation dose to the target and by protecting the proximate healthy tissue from harm [1], [2].

Prostate motion may occur in between (inter-fraction) or during (intra-fraction) radiation therapy treatments. As the prostate is not observable on kV projection images one technique employed for verifying the prostate's location involves implanting fiducial markers into the prostate. Extraction of the markers' positions on kV images allows for computing a 3D model of the markers and thereby following the movement of the prostate. Use of fiducial markers has been shown to be successful for inter-fraction prostate motion management through precise pre-treatment tumor localization [1], [2], [3]. A more challenging task, however, is tumor tracking for intra-fraction prostate motion. This calls for a robust and accurate marker segmentation algorithm implementable in real-time.

Manuscript received November 22, 2013.

S. B. and J. L Authors are with Oakland University, Rochester, MI.

L. Z. is with William Beaumont Hospital, Royal Oak, MI.

Many of the previous works on this subject suggest detection methods that rely on template matching approaches and require a priori knowledge of the markers' dimension and geometry. In [4], Nederveen proposed on such method where cylindrical markers were located by convolving the acquired images with rectangular marker extraction kernel (MEK) templates created after learning the markers' size and orientation at lateral and anterior-posteriors views. Buck et al. in [5] suggested a comparable method by replacing application of MEK for marker extraction with a Mexican Hat Filter. Cross-correlation based methods have also been developed. Similar to template matching techniques they necessitate a priori knowledge. In [6], the authors identify the markers by using cross-correlation between the images and previously acquired images from earlier treatments. The feasibility of these three methods was analyzed in [1]. The authors reported close performance results for the two template matching techniques and found the cross-correlation approach to have the highest detection accuracy rate. In our study, application of the template matching techniques is complicated by the varying geometry of the fiducial markers used. Linear fiducial markers appear as lines with irregular curvatures on kV images and for this reason designing a standard template is not feasible. In the collected kV images, marker extraction by normalized cross-correlation demands image pre-processing steps that can be encumbering. Additionally, the authors in [1] observed greater failure in correct marker detection in the lateral viewing angles in all three methods and attributed it to interference from boney tissue and proximity of the markers on the images.

In this paper, an automated method for visi-coil (IBA Dosimetry, Bartlett TN) fiducial marker detection based on fast marching approach is presented. In Section II, the background information of fast marching method and the forward projection technique will be discussed. Section III will cover the proposed method of fiducial marker segmentation on kV images and their 3D reconstruction. Finally, Sections IV and V will be devoted to the discussion of results and the conclusion.

978-1-4799-0534-8/13/$31.00 ©2013 IEEE

II. Background

A. Fast marching method

Fast marching algorithm (FMM) was introduced by Sethian in 1996 and is closely related to Dijkstra's shortest path algorithm [7], [8]. On a gray scale image denoted by $\pi = [0,1]^2$, a smooth path, $\gamma(t): [0,1] \rightarrow \pi$, connecting two points x_s and x_e can be characterized by a differentiable continuous curve with approximately constant intensity value. The geodesic curve, or the shortest path, connecting $x_s = \gamma(0)$ and $x_e = \gamma(1)$ can be segmented by finding the path with the minimum length $L(\gamma)$ where

$$L(\gamma) = \int_0^1 W(\gamma(t))\|\gamma'(t)\|dt \quad (1)$$

and

$$W(x) = |f(x) - f(x_e)| + \varepsilon \quad (2)$$

$f(x)$ is the intensity value of the image at point x, ε is a small constant value and $W(x)$ defined in this way is a simple regularizing weight matrix that generates a smaller $L(\gamma)$ when the path's intensity value is closer to $f(x_e)$.

The problem of $L(\gamma)$ minimization, i.e. finding the shortest path, can be transformed into the solution of the isotropic Eikonal Equations given by

$$\|\nabla u(x)\| = \tau(x), \; x \in \pi \quad (3)$$

$$u(x) = 0, \qquad x \in \partial\Omega \quad (4)$$

where τ is the speed function of the front wave propagating outward, Ω is the domain and $\partial\Omega$ is the segmentation region's boundary [7], [8].

We let $\tau(x) = W(x)$, $\partial\Omega = \{x_s\}$ and $\|.\|$ be the Euclidean distance. The solution, $u(x)$, is the geodesic distance from x_s to x_e. Computation of $u(x)$ can be done quickly through the FMM with complexity of $O(Nlog(N))$. A MATLAB toolbox implementation of the FMM written by Gabriel Peyre is available on MATLAB Central and is applied in our algorithm [8].

B. Forward projection

The proposed segmentation method in this work relies on projecting an initial 3D model of fiducial markers onto the kV projection images. The forward projection algorithm follows the approach delineated in [9]. It is explained below.

A projection plane, **k**, is described by its system geometry of three normal vectors, e_ξ, e_u and e_v in the z, y and x direction and an origin, D. e_u and e_v point along the height and width of **k** while e_ξ is aligned with the optical axis. Given a 3D voxel, its corresponding pixels on **k** can be found in two successive steps by first calculating the projected pixels in 3D at **k** according to (4) and then completing a forward projection on **k** by following (5) and (6).

$$P(x^{3D}) = \left(\frac{(D-F).e_\xi}{(x^{3D}-F).e_\xi}\right).(x^{3D} - F) + F \quad (4)$$

$$v(x^{3D})_u = (\, P(x^{3D}) - D).e_u.\frac{P_u}{w_u} \quad (5)$$

$$v(x^{3D})_v = (\, P(x^{3D}) - D).e_v.\frac{P_v}{w_v} \quad (6)$$

where p_u, p_v, w_u, w_v are the detection plane height, width in pixels and detection plane height, width in mm respectively, F is the 3D coordinate position of the pinhole camera, and x^{3D} is the 3D coordinate of the voxel.

III. Marker segmenation and 3D reconstruciton

In this study the patient was implanted with 3 linear visi-coil fiducial markers 3 mm in diameter and 20 mm in length. During the treatment session, 761 kV projection images over 360 degrees rotation of the gantry were collected in 2 minutes using a 512×512 pixel projection plane with pixel resolution of .518×.518 mm^2. For simpler processing, the images were cropped into 120×120 pixel cuts centered at the iso-center. Our marker segmentation process consists of four basic steps:

1. 3D model re-projection onto the kV projection images;
2. Estimation of the seed and termination point coordinates on the projection image for each visi-coil;
3. Bounding the search region around each marker;
4. Performing marker detection by FMM;

The algorithm searches for a single visi-coil at a time. In advance, a 3D model of visi-coils is extracted by thresholding CT images captured before treatments. At each projection angle, the 3D model is adopted as a reference and re-projected onto the kV images by the abovementioned forward projection technique.

A. Finding End Points

A drawback of the fast marching method is its requirement for the operator to manually provide the start and end point of each visi-coil. The new 2D re-projection points from the 3D reference model can be exploited to overcome this limitation. They supply information about the orientation of the markers at each viewing angle. The endpoints of the sequence of 2D re-projections points corresponding to a marker can easily be identified. Let *d* denote one of the end points. We define a region of interest (ROI) with area of 5×5 pixels around *d* and search within ROI for the most likely end point.

Contrast enhancement by histogram equalization followed by thresholding is performed on ROI. The potential end point must be the end point of a continuous line with same direction as that of the matching marker found from the 2D re-projection points. This implies that an isolated high intensity point will not be picked out as the potential end point.

B. Marker Extraction by FMM

Once start and end points of a visi-coil marker are spotted, based on the 2D re-projection points a boundary is defined. This boundary outlines the region where the fast marching method will seek out the shortest path and is the neighborhood of all the 2D re-projection points, the specified start and the end points with a distinct margin. Mapping a boundary region aims to prevent the FMM path from veering off into nearby high intensity value pixels in low quality kV images and especially when the visi-coil projections rest in close proximity of boney anatomy. At this point, visi-coil marker segmentation on kV projection images is realized through the fast marching method by detecting the shortest path within the bounded region and between the given start and end points.

C. 3D Reconstruction

3D reconstruction of the visi-coil markers from the segmentation results on a sequence of kV images is accomplished via the point-based curve reconstruction algorithm offered in [10]. The algorithm aims to minimize a cost function given in (7) through an iterative process by adjusting the coordinates of the 3D curve in space such that the error between the 2D curves and the re-projection curves is decreased. In this method the sequence of selected frames are divided into two groups called reference and non-reference curves. The error measured between a re-projected point, $\hat{x}_k$, and a point on the reference and non-reference curve is shown in Fig. 1. $[\overline{u}_{r\,k}, \overline{v}_{r\,k}, 1]^T$ denotes the homogenous coordinates of the kth 2D points on the reference curves, on the rth view. Points on the reference curves are fixed in space. Similarly, $[u_{i\,k}, v_{i\,k}, 1]^T$ denotes the homogenous coordinates of the kth 2D points on the non-reference curves, on the ith view. Unlike the reference points, the non-reference points are free to move along the 2D curves.

$$\min_{P,X,\lambda,x} \left\{\sum_{(r,k)\in \boldsymbol{R}}\left[\left(\overline{u}_{r\,k}-\frac{P_r^1 X_k}{\lambda_{r\,k}}\right)^2+\left(\overline{v}_{r\,k}-\frac{P_r^2 X_k}{\lambda_{r\,k}}\right)^2\right]\right.$$
$$\left.\sum_{(i,k)\in \boldsymbol{A}\backslash\boldsymbol{R}}\left[\left(u_{i\,k}-\frac{P_i^1 X_k}{\lambda_{i\,k}}\right)^2+\left(v_{i\,k}-\frac{P_i^2 X_k}{\lambda_{i\,k}}\right)^2\right]\right\} \qquad (7)$$

subject to

(a) $x_{i\,k} = [u_{i\,k}\; v_{i\,k}\; 1]^T \in c_i\,,\;\; (i,k) \in \boldsymbol{A}\backslash\boldsymbol{R}$

(b) $\lambda_{i\,k} = P_i^3 X_k,\;\; (i,k) \in \boldsymbol{A}$

$\frac{P_r^i X_k}{\lambda_{r\,k}}$ in (7) finds the ith 2D coordinates of the re-projected curve from the kth 3D point, X_k, where P_r is the projection matrix corresponding to viewing angle r, and λ_r is the depth of X_k along the optical axis. c_i is the ith non-reference curve. $\boldsymbol{R}$ and $\boldsymbol{A}$ represent the set of all reference and all representative 2D points. In our algorithm, the 2D re-projection points were computed by forward projection method described in section II.B.

Prostate motion monitoring can be achieved by real-time 3D reconstruction of the fiducial markers. This step is to be complete later. In this paper, we only present a static 3D reconstruction of visi-coil markers.

IV. Results and Discussion

A. Segmentation Results

Out of 761 obtained kV images, 406 were marker visible. In Fig. 2 segmentation results are presented. In the left panel the original image is depicted. On the right, the three detected visi-coil markers are shown with the solid blue line. The green dots are the re-projection reference point. The red stars are the detected end points of each visi-coil and the solid red dots signify the corners of the rectangular ROI where we search for the possible end points.

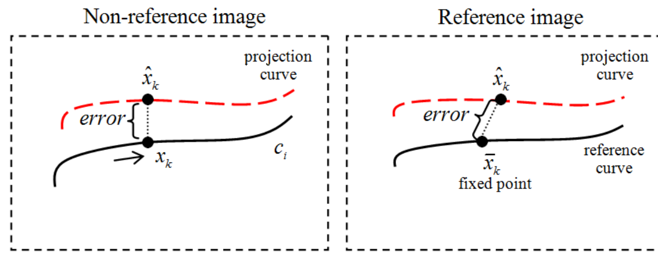

Fig. 1. Reference and non-reference curves used in 3D reconstruction.

At certain kV projection angles, the presence of high intensity value boney structure in the proximity of visi-coils can hinder their correct segmentation [1]. One contributing factor to this problem arises from reduced intensity contrast between the markers and the background due to boney tissue occlusion. This effect can be seen in the original image of Fig. 3. On the right hand side the detection results in this case are shown. Another complicating factor under such projection angles, noticeable in the FMM detection, is the cross-over between the markers and the decreased inter-marker distance that can deter correct end point detection and can also cause the FMM path to drift from one visi-coil to another.

With the guidance of 3D re-projections, visi-coil segmentation accuracy can be enhanced when the marker is partially blurred due to noise, as demonstrated in Fig. 4, or 5. The far right marker in Fig. 4, brings into attention the difficulty of automated detection of visi-coil end point. When the end points are not clearly defined, background noise or boney tissue may be incorrectly selected.

B. 3D reconstruction results

Following the procedure outlined in section III.C and using the segmentation results from marker extraction by FMM, a static 3D model of the visi-coil fiducial markers is computed. A plot of the new 3D model against the original 3D model extracted from CT images by thresholding can be seen in Fig. 6. Four non-reference images and a single reference image were chosen. From each non-reference curve 50 points at equally spaced intervals were collected as part of the representative points. The 3D reconstruction outcome shows a smoother and more continuous curve for each of the markers. For assessment this model was projected on to a kV image. The result can be seen in Fig. 7.

V. Conclusion

An automated fast marching based approach for visi-coil fiducial marker detection in kV projection images was presented. Using this method can yield more robust and accurate detection under noisy condition and consequently lead to a smoother 3D reconstruction model. In the future, we wil incorporate the 3D reconstruction algorithm and the automated fiducial marker detection algorithm for real-time motion tracking during prostate cancer radiation therapy.

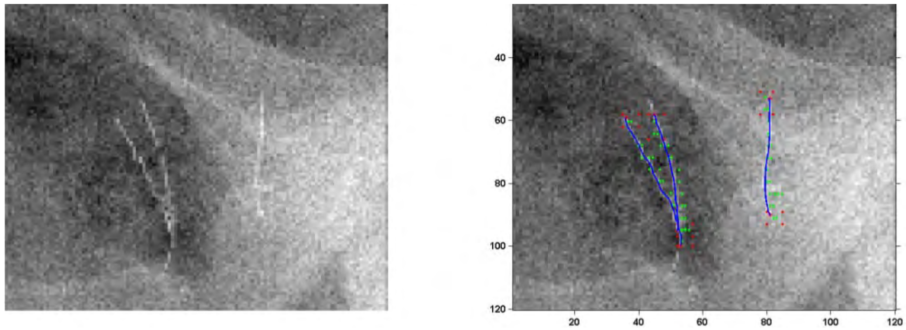

Fig. 2. Fiducial marker detection results on kV image at an oblique view.

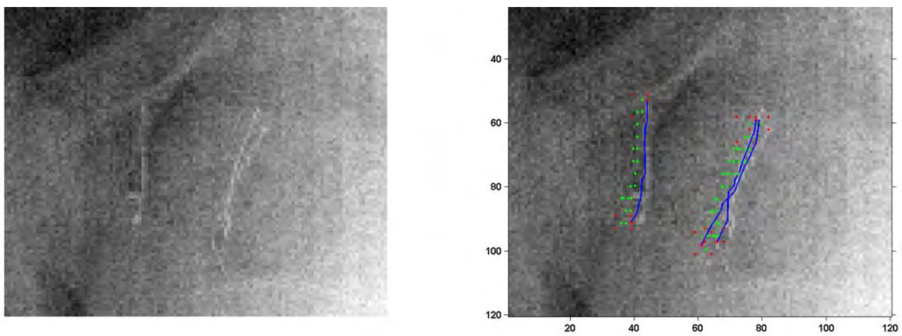

Fig. 3. Detection at extreme oblique angles in the presence of boney tissue interference.

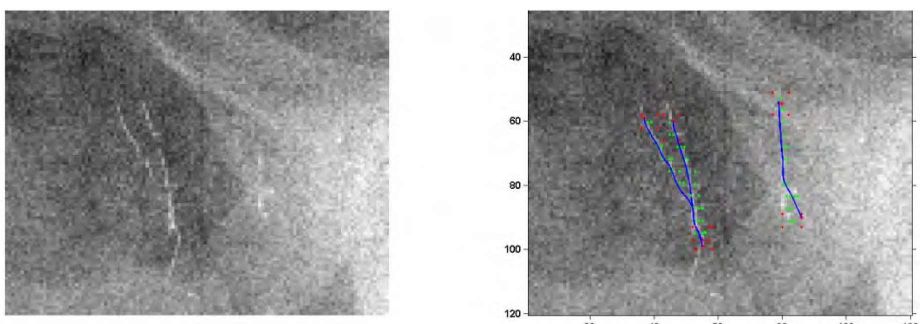

Fig. 4. Only the lower end portion of the far right visi-coil is discernible in the original image.

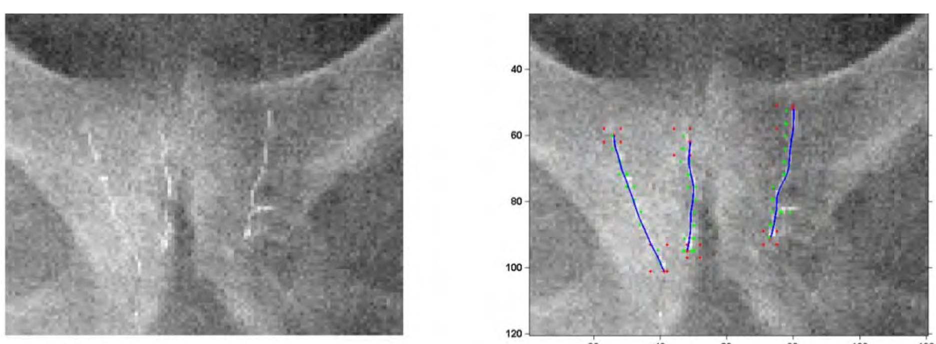

Fig. 5. Marker on the far left lies on top of pelvis bone in the image and is not easily spotted.

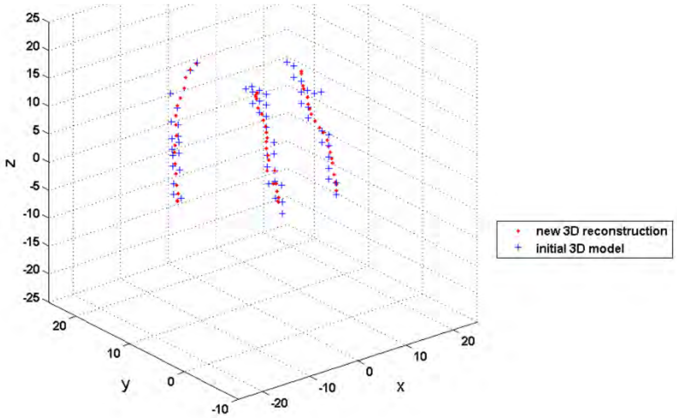

Fig. 6. 3D reconstruction of fiducial markers and the initial 3D model.

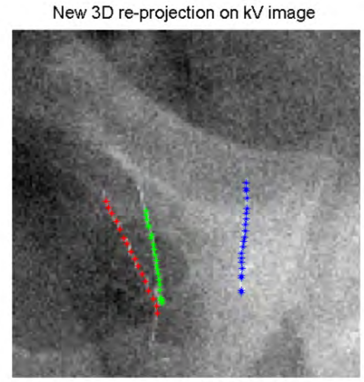

Fig. 7. New 3D reconstruction re-projected onto the kV image.

REFERENCES

[1] Harris, E.J., McNair, H.A., Evans, P., "Feasibility of full automated detection of fiducial markers implanted into the prostate using electronic portal images: A comparison of methods", *Int. J. Radiation Oncology Biol. Phys.*, vol. 66, no. 4, 1263-1270, 2006.

[2] Slagmolen, P. Hermans, J. Maes, F., Budiharto, T. Haustermans, K., van den Heuvel, F., "Fast, accurate and robust automatic marker detection for motion correction based on oblique kV or MV projection image pairs", *Med. Phys.*, vol. 37, no. 4, 1554-1564, 2010.

[3] Huang, E. Dong, L., Chandra, A., Kuban, D.A., Rosen, I.I., Evans, A., Pollack, A., "Intrafraction prostate motion during IMRT for prostate cancer", *Int. J. Radiat. Oncol. Biol. Phys.*, vol. 53, no. 2, pp. 261-268, 2002.

[4] Nederveen, A., Lagendjik, J.J.W., Hofman, P., "Detection of fiducial gold markers for automatic on-line megavoltage position verification using a marker extraction kernel (MEK)". *Int. J. Radiat. Oncol. Biol. Phys.*, vol. 47, pp. 1453-1442, 2000.

[5] Buck, D., Alber, M., Nusslin, F, "Potential and limitations amorphous silicon flat-panel imager", *Phys. in Med. and Biol.*, 48, pp. 763-764 (2003)

[6] Balter, J., Lam, K.L., Sandler, H.M., Littles, J.F., Bree, R.L., Ten Haken, R. K., "Automated localization of the prostate at the time of treatment using implanted radiopaque markers: Technical feasibility", *Int. J. Radiat. Oncol. Biol. Phys.*, vol 33, no. 5, pp. 1281-1286 (1995)

[7] Sethian J.A., "A fast marching level set method for monotonically advancing fronts", *Proceedings of the National Academy of Sciences of the United States of America*, 93, 1591-1595, 1996.

[8] Peyre, G.: Toolbox Fast Marching, On MATLAB Central. http://www.mathworks.com/matlabcentral/fileexchange/6110-toolbox-fast-marching (2009), Accessed 21 Dec. 2012

[9] Jandt, U., Schafer, D., Grass, M., Rasche, V., "Automatic generation of 3D coronary artery centerlines using rotational X-ray angiography", *Medical Image Analysis*, 13, 846-858, 2009.

[10] Mai, F., Hung, Y.S., "3D Curves Reconstruction from Multiple Images", *International Conference on Digital Image Computing: Techniques and Applications*, 462-467, 2010.